

Document downloaded from:

<http://hdl.handle.net/10251/83162>

This paper must be cited as:

Liu, L.; Concepción Heydorn, P.; Corma Canós, A. (2016). Non-noble metal catalysts for hydrogenation: A facile method for preparing Co nanoparticles covered with thin layered carbon. *Journal of Catalysis*. 340:1-9. doi:10.1016/j.jcat.2016.04.006



The final publication is available at

<http://doi.org/10.1016/j.jcat.2016.04.006>

Copyright Elsevier

Additional Information

**Non noble metal catalysts for hydrogenation: a facile method for
preparing Co nanoparticles covered by thin layered carbon**

Lichen Liu, Patricia Concepcion and Avelino Corma*

*Instituto de Tecnología Química, Universidad Politécnica de Valencia-Consejo Superior de
Investigaciones Científicas (UPV-CSIC), Av. de los Naranjos s/n, 46022 Valencia, Spain*

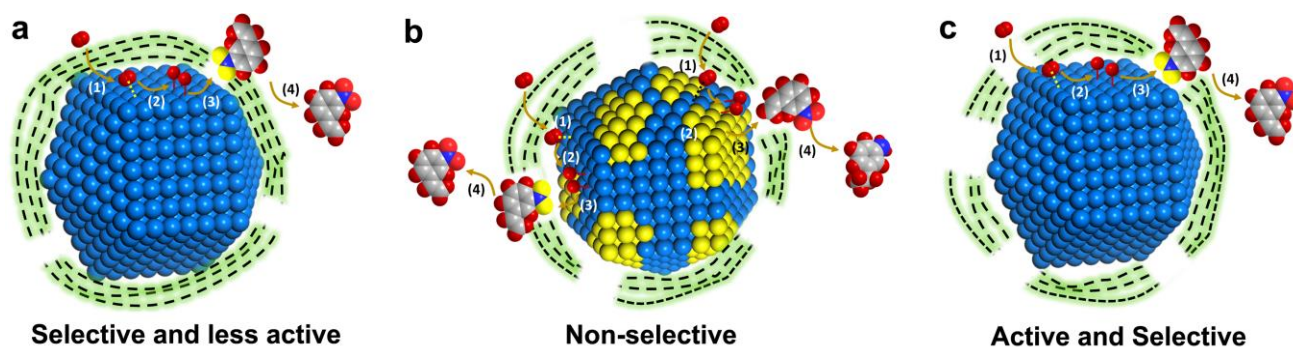
*Corresponding author: acorma@itq.upv.es (A.C.)

Abstract

Metallic cobalt nanoparticles with surface CoOx patches covered by thin layered carbon (named as Co@C), have been directly synthesized by thermal decomposition of Co-EDTA complex. Raman spectra and HRTEM images suggest that discontinuities can be found in the disordered layered carbon. XPS shows that the CoOx patches in the Co@C nanoparticles can be reduced to metallic Co by H₂ under reaction conditions (7 bar at 120 °C), and H₂-D₂ exchange experiments show that the reduced metallic Co nanoparticles covered by carbon layers can dissociate H₂. The Co@C nanoparticles show excellent activity and selectivity during chemoselective hydrogenation of nitroarenes for a wide scope of substrates under mild reaction conditions. Based on the results from DRIFTS adsorption experiments, we propose that metallic Co in the Co@C nanoparticles is the active phase. The role of the carbon layers is to protect the Co from over-oxidation by air, leading to the chemoselective hydrogenation of nitroarenes.

Keywords: Co nanoparticle, Layered Carbon, Chemoselective Hydrogenation, Nitroarenes

Graphic Abstract



Highlights

- Metallic Co nanoparticles covered by thin carbon layers are prepared.
- Metallic Co is the active phase for hydrogenation reaction.
- The role of carbon layers is to protect Co nanoparticles from over-oxidation.
- Surface properties of Co nanoparticles affect the chemoselectivity.

1. Introduction

The chemoselective hydrogenation of nitroarenes is an important hydrogenation reaction for production of fine and bulk chemicals with wide industrial and pharmaceutical applications.¹ Noble metals such as Au, Pt, Ru, Pd, Ir have been proved to be active components for hydrogenation of nitroarenes.^{2,3} By controlling the metal-support interaction and particle size, the chemoselective hydrogenation of nitroarenes can be carried out with high chemoselectivity.^{4,5} However, considering the high price and limited availability of noble metals, it is of interests to develop non-noble metal catalysts for chemoselective hydrogenation reactions.

In the last years, non-noble metal catalysts have attracted much attention due to their comparable properties with noble metal catalysts in photocatalysis, electrocatalysis, and in homogeneous and heterogeneous catalysis.⁶⁻⁹ Recently, the applications of CoO_x@N-doped carbon and Fe₂O₃@N-doped carbon materials for chemoselective hydrogenation of nitroarenes has been reported.^{10,11} In their works, the catalysts work under high-pressure conditions (50 bar of H₂), and the authors claimed that metal oxide nanoparticles covered by carbon layers were thought to be the active species for the chemoselective hydrogenation and hydrogenation-transfer reaction. In a recent paper, Wang et al. observed the *in situ* transformation of CoO_x to metallic Co during the selective hydrogenation of nitroarenes under 30 bar of H₂, although the catalyst was a mixture of CoO_x and metallic Co.¹² As substitutes for noble metal catalysts, the non-noble metal catalysts should work under similar conditions like Pt (3-6 bar of H₂) and Au (9-15 bar of H₂) catalysts. However, the reported catalysts are working under much higher H₂ pressure than noble metal catalysts.

And from the above reports, it's still not clear whether metallic Co or CoO_x is the active phase for the selective hydrogenation reaction. Moreover, if one considers that *in situ* dynamic transformation of metal species can occur under reaction conditions, the real active species in the hydrogenation reaction may not be the starting materials. Furthermore, the role of the layered carbon materials in the catalytic mechanism during those catalytic hydrogenation has not been clarified. In some works, the carbon layers can protect metal NPs. For example, Ding et al. prepared supported Ni NPs embedded in carbon nitride layers for hydrogenation of nitrobenzene under strong acid condition.¹³ The carbon layers may also block the accessibility of substrates to the metal NPs. In some previous works,¹⁰⁻¹² it was proposed that the hydrogenation reactions occur on the surface of carbon layers.

However, considering the impermeability of graphene, H₂ cannot diffuse directly through perfect graphene layers making even more difficult to unveil the role of carbon layers in hydrogenation reactions.^{14,15}

In the first part of this work, by following the thermal decomposition of a Co-EDTA complex, we prepare monodispersed Co nanoparticles with a thin carbon shell (Co@C). Compared with conventional method for monodispersed Co nanoparticles, organic ligands are not required here to stabilize the Co nanoparticles. The resultant material can catalyze the chemoselective hydrogenation of nitroarenes under mild reaction conditions similar to Au catalysts (7-10 bars of H₂) with high activity and selectivity (> 93%). In the second part of this work, with the help of *in situ* spectroscopic characterizations, we will show that the selective adsorption of reactants occurs on the surface of cobalt nanoparticles. Metallic Co, instead of CoO_x, is the active phase for hydrogenation reaction and the role of the carbon layers is to protect the metallic Co NPs from over-oxidation.

2. Experiments

Preparation of Co@C NPs. The Co@C NPs were prepared through the reduction of Co-EDTA complex by H₂. The Co-EDTA complex were prepared through a hydrothermal process. First, 6.98 g Co(NO₃)₂, 4.47 g Na₂EDTA and 0.96 g NaOH are dissolved in 20 mL H₂O. Then, 10 mL methanol was added to the mixed aqueous solution temperature under stirring at room temperature. After the formation of a homogeneous solution, 23 mL of the purple solution was transferred into a 35 mL stainless steel autoclave followed by static hydrothermal processing at 200 °C for 24 h. After cooling to room temperature, the generated precipitates were filtered and washed with deionized water and acetone several times followed by drying at 100 °C in air for 16 h. The obtained complex was denoted as Co-EDTA. Then, Co@C NPs were prepared by reduction of Co-EDTA in H₂ (50 mL/min) at 450 °C for 2 h with a ramp rate of 10 °C/min from room temperature to 450 °C. After the H₂ reduction process at 450 °C, the sample was cooled down to room temperature in H₂ atmosphere. Then the black solid product was stored in a glass vial in ambient environment. The ICP analysis shows that the amount of cobalt in the Co@C NPs is ≥ 95 wt%. The Co@C-250Air and Co@C-450Air were prepared through the calcination of Co@C sample in air (50 mL/min) at 250 and 450 °C for 2 h with a ramp rate of 5 °C/min, respectively.

Catalytic studies. The chemoselective hydrogenation of nitroarenes was performed in batch reactors. The reactant, internal standard (dodecane), solvent (toluene or THF), powder catalyst as well as a magnetic bar were added into the batch reactor. After the reactor was sealed, air was purged by flushing two times with 10 bar of hydrogen. Then the autoclave was pressurized with H₂ to the corresponding pressure. The stirring speed is kept at 800 rpm and the size of the catalyst powder is below 0.02 mm to avoid either external or internal diffusion limitation. Finally, the batch reactor was heated to the target temperature. For the kinetic studies, 50 μ L of the mixture was taken out for GC analysis at different reaction time. For the scope studies, 100 μ L of the mixture was taken out for GC analysis. The products were also analyzed by GC-MS.

Characterization techniques. Samples for electron microscopy studies were prepared by dropping the suspension of Co@C NPs using CH₂Cl₂ as the solvent directly onto holey-carbon coated Nickel grids. All the measurements were performed in a JEOL 2100F microscope operating at 200 kV both in transmission (TEM) and scanning-transmission modes (STEM). STEM images were obtained using a High Angle Annular Dark Field detector (HAADF), which allows Z-contrast imaging.

Field-emission scanning electron microscopy (FESEM) measurement is performed with a ZEISS Ultra 55 FESEM. The solid powder sample was adsorbed on conductive carbon tape.

X-ray photoelectron spectra of the catalysts were recorded with a SPECS spectrometer equipped with a Phoibos 150MCD-9 multichannel analyzer using non monochromatic MgK α (1253.6 eV) irradiation. Spectra were recorded using analyser pass energy of 30 eV, an X-ray power of 100W and under an operating pressure of 10⁻⁹ mbar. The fresh Co@C NPs sample was reduced by H₂ (7 bar) at 120 °C for 60min in a high pressure catalytic cell connected, under ultra-high vacuum, to the XPS analyze chamber. Peak intensities have been calculated after nonlinear Shirley-type background subtraction and corrected by the transmission function of the spectrometer. During data processing of the XPS spectra, binding energy (BE) values were referenced to C1s peak (284.5 eV). CasaXPS software has been used for spectra treatment.¹⁶

Raman spectra were recorded at ambient temperature with a 785 nm HPNIR excitation laser on a Renishaw Raman Spectrometer (“Reflex”) equipped with an Olympus microscope and a CCD

detector. The laser power on the sample was 15mW and a total of 20 acquisitions were taken for each spectra.

Hydrogen /deuterium (H/D) exchange experiments were carried out in a flow reactor at 25 and 80 °C. The feed gas consisted of 4 mL/min H₂, 4 mL/min D₂ and 18 mL/min argon, and the total weight of catalyst was 180 mg. Reaction products (H₂, HD and D₂) were analysed with a mass spectrometer (Omnistar, Balzers). The Co@C sample has been *in situ* reduced at 450 °C for 2 h with a ramp rate of 10 °C/min from room temperature to 450 °C. Then the temperature was decreased to 25 °C and, once stabilized, the H₂ feed was change to the reactant gas composition. The temperature was increased to 80 °C and maintained at 80 °C for 1 h.

DRIFT spectra were recorded at room temperature with a Nexus 8700 FTIR spectrometer using a DTGS detector and acquiring at 4 cm⁻¹ resolution. Prior to the adsorption experiments, the ex situ reduced samples was *in situ* reduced at 120 °C in H₂ atmosphere for 2 h. After activation the sample was evacuated at 10⁻² mbar and nitrobenzene and/or styrene adsorbed until sample saturation followed by evacuation (10⁻² mbar) in order to remove physisorbed species. A commercial DRIFT cell (SPECAC) has been used. Spectra were acquired in Kubelka-Munk units.

Powder X-ray diffraction (XRD) was performed in a HTPhilips X'Pert MPD diffractometer equipped with a PW3050 goniometer using Cu K α radiation and a multisampling handler.

3. Results and discussions

3.1 Catalyst preparation and characterization

The Co@C NPs were prepared by thermal decomposition of Co-EDTA complex in H₂ atmosphere at 450 °C. The morphological characterization of Co-EDTA complex can be found in supporting information (see **Fig. S1**). The morphology of Co@C NPs was characterized by FESEM and TEM. As it is shown in **Fig. S2** and **Fig. 1a**, the Co@C material is formed by monodispersed metal NPs ranging from ca. 20 nm to ca. 150 nm. Those Co NPs are covered by carbon layers with thickness ranging from ca. 1 nm to ca. 10 nm (**Fig. 1b**). From the HRTEM images (**Fig. 1c** and **Fig. 1d**), the lattice fringe of metallic Co can be seen.¹⁷ A further look to the surface structures of the Co NPs allows to observe the crystal lattice fringes of Co₃O₄, as shown in **Fig. S3**.¹⁸ Therefore, one can assume, in a first approximation, that the Co NP can be formed by a core-shell structure with metal

Co at the core and CoO_x as the shell. In order to know the chemical composition of the Co@C sample, STEM-HAADF elemental mapping was performed and the results are displayed in **Fig. 1g** to **1j**. They confirm that Co NPs are covered by carbon layers. Meanwhile, oxygen can also be found in the sample, that may come from surface CoO_x and/or from the oxygenated groups in carbon layers. Contrast profiles of the carbon layers over Co NPs were also obtained, as presented in **Fig. 1e** and **Fig. 1f**. It can be seen there that the distance between the carbon layers is 0.34-0.37 nm, which corresponds to the distance between graphene layers. The thickness of most carbon layers are between 1 nm and 5 nm, with several layers of graphene.¹⁹ A schematic illustration about the structure of Co@C NP is shown in **Fig. 1k**, indicating that the particle contains metallic Co as the core as well as some CoO_x patches on the surface and carbon layers surrounding.

From the HRTEM images (**Fig. S4** to **Fig. S6**), it can also be seen that the thin carbon layers over Co NPs are not closed and some cracks can be found, implying that reactant molecules can have access to the Co NPs through the carbon layers. This can explain why the Co@C NPs could be partially oxidized by air in ambient condition after the preparation procedure. In a recent work of Bao and his co-workers, they have prepared a sample with CoNi alloy NPs totally encapsulated by several layers of graphene.²⁰ Those CoNi NPs are not soluble in a strong acid environment due to the protection effect of the carbon layers. However, in our case, Co NPs covered by cracked carbon layers can be almost totally dissolved in aqueous H₂SO₄ (photographs of the dissolving process can be seen in **Fig. S7**), suggesting that Co@C NPs are not totally covered by carbon layers.

In general, due to the instability of metallic Co NPs, their preparation for heterogeneous catalytic application still remains a challenge. So far, metallic Co NPs are usually prepared through wet-chemistry method.²¹⁻²³ In those methods, Co NPs are capped by organic ligands to protect them from agglomeration and oxidation by air, but, at the same time, these long-chain organic ligands decrease the activity of Co NPs. Furthermore, Co NPs prepared from wet-chemistry methods are usually not stable in ambient conditions due to the oxidation of Co by air. In contrast, with the protection effect of carbon layers, the Co NPs prepared by our method can be stored under ambient conditions for over one month without obvious morphological changes. Only the oxidation of Co NPs at the surface occurs and CoO_x patches are formed that can be easily reduced by H₂ to metallic Co. Compared with previous reported pyrolysis methods (calcination at 800 °C), well-defined Co@C

NPs with carbon layers can be directly synthesized at relatively lower temperature. These air-stable Co@C NPs with CoO_x patches can be prepared in large scale (several grams) in a facile way.

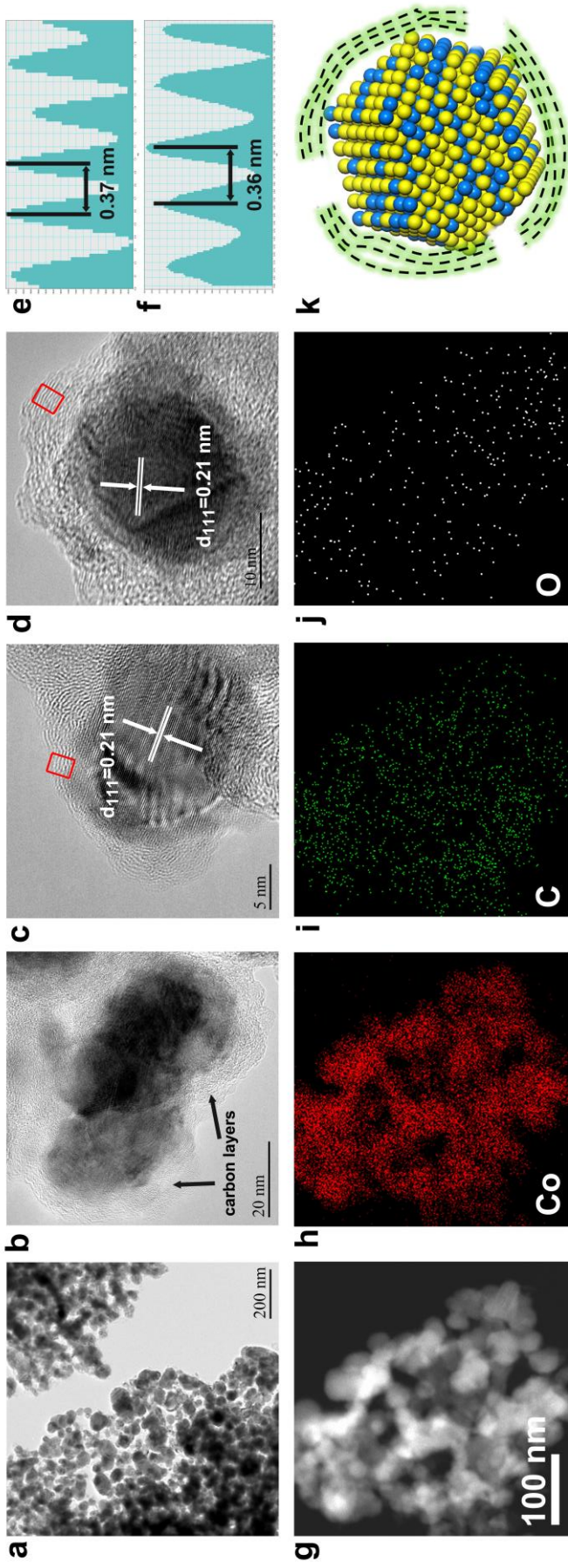


Fig. 1. Morphological characterizations of Co@C NPs. (a, b) Low-magnification TEM image of Co@C. The size of Co NPs ranges from ca. 20 to ca. 150 nm. Monodispersed Co NPs are separated by carbon layers, as show in (b). (c, d) HRTEM images of Co NPs covered by carbon layers. (e, f) Profile of the carbon layers in selected areas in c and d, respectively. The distance between two carbon layers is about 0.36-0.37 nm. (g) STEM-HAADDF image of Co@C NPs. (h-j) Elemental mapping of Co, C and O. (k) Schematic illustration of the structure of Co@C NPs. Blue balls stands for metallic Co and yellow balls stands for CoOx. The surface of Co NP is mainly made of CoOx while the core is metallic Co. The green circle surrounding the particle is the carbon layers with cracks.

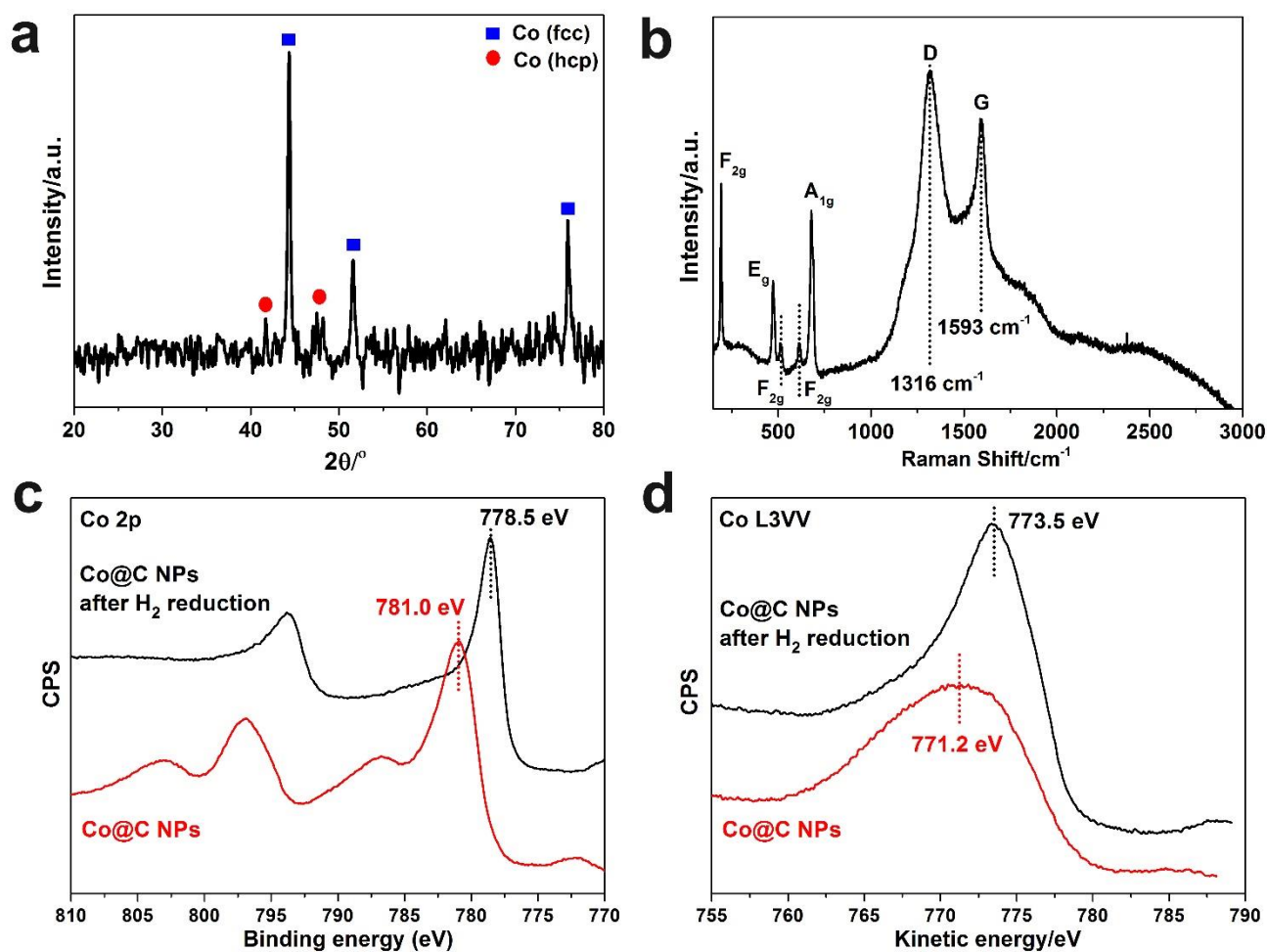


Fig. 2. Structure characterizations of Co@C NPs. (a) XRD pattern of fresh Co@C NPs, (b) Raman spectrum of Co@C NPs, XPS spectra of Co 2p region (c) and Co L3VV Auger spectra (d) of the fresh Co@C NPs and the sample after *ex situ* reduction by 7 bar of H₂ at 120 °C.

The bulk and surface properties of the Co@C NPs were also investigated. The XRD pattern of Co@C NPs is shown in **Fig. 2a**. Only the X-ray diffraction patterns of metallic Co can be observed with no X-ray diffraction peaks corresponding to other species, although the formation of CoOx patches could be observed by HRTEM. The fact that CoOx is not detected by XRD should be due to the low amount of CoOx patches in the Co@C sample. In the case of metallic Co, besides the cubic Co phase (PDF code: 96-900-8467), a small amount of hexagonal Co phase (PDF code: 96-900-8493) can also be observed in the XRD pattern. For metallic Co, the hexagonal-closed packed (*hcp*) phase is more stable at lower temperature than the face-centered cubic (*fcc*) phase.²⁴ Since the Co-EDTA complex was decomposed and reduced at 450 °C, it is not surprising to see that both phases can exist.²⁵

The surface structures of Co@C NPs as well as the carbon layers were also studied by Raman spectroscopy. As it is indicated in **Fig. 2b**, vibration modes of Co₃O₄ (F_{2g}, E_g and A_{1g}) can be observed.²⁶ Besides, the typical Raman signals of layered carbon, bands at 1318 cm⁻¹ and 1595 cm⁻¹, can be observed, which are corresponding to *D* and *G* band, respectively.²⁷ No peak related to **2D** band is detected between 2500 and 2800 cm⁻¹. The intensity ratio of G band (I_G) to D band (I_D) is ca. 0.8, suggesting that there is a large percentage of disorder in the structured carbon in Co@C NPs.²⁸ Combing these results and those from HRTEM images, it can be speculated that the degree of graphitization is relatively low in the carbon layers around Co NPs. Therefore, based on the structural characterizations, we can propose that Co@C NPs have core-shell structures with metallic Co as the core, CoOx on the surface of Co crystallites and thin layered carbon as the shell.

X-Ray photoelectron spectroscopy (XPS) was employed to study the chemical state of Co in the as-prepared Co@C NPs. The Co@C NPs were reduced by H₂ at 7 bar and 120 °C (That condition will also be used in the hydrogenation reaction.) within a pre-reactor integrated to the apparatus and the sample is maintained isolated from any external contact during all the process. The XPS spectra of Co 2p region and Auger spectra of Co L3VV are shown in **Fig. 2c** and **Fig. 2d**, respectively. In the as-prepared Co@C sample, only CoO_x can be observed, which can be ascribed to the CoOx patches on the surface of Co NPs.²⁹ After H₂ reduction treatment (7 bar of H₂ at 120 °C), the CoOx is totally transformed into metallic Co, as confirmed by both Co 2p XPS and Co L3VV Auger spectra. In the

fresh as-prepared catalyst, N is presented in the sample, as shown by elemental mapping (see **Fig. S8**). However, after the *ex situ* reduction treatment, no N can be found in the sample by XPS, indicating that there is practically no N species in the working catalyst.

With the characterization results presented up to now, we can say that during preparation of Co@C NPs, Co NPs of 20-150 nm were generated which are formed by a metallic Co core with CoOx on the surface that are surrounded by disordered carbon layers. Moreover, under reduction conditions, that are the same used for performing the catalytic test, the CoOx patches can be totally reduced to metallic Co.

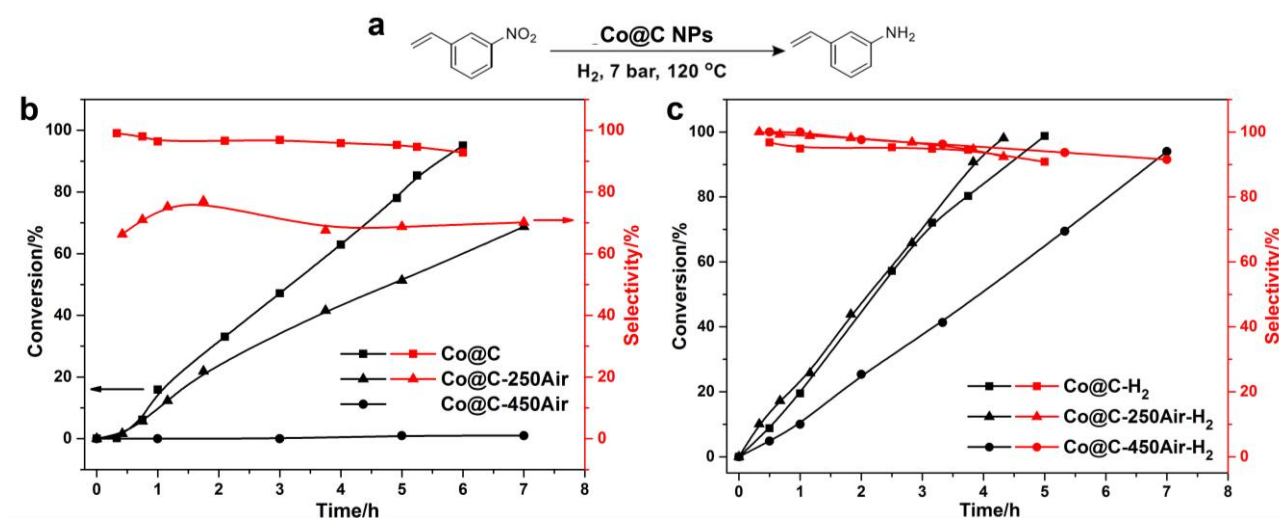


Fig. 3. (a) Reaction scheme of the chemoselective hydrogenation of 3-nitrostyrene. Reaction conditions: 0.5 mmol 3-nitrostyrene, 30 mg Co@C NPs as the catalyst, 2 mL toluene as solvent, 30 μ L dodecane as the internal standard. (b) Catalytic performances of Co@C, Co@C-250Air and Co@C-450Air in chemoselective hydrogenation of 3-nitrostyrene to 3-aminostyrene. The black legends and red legends correspond to conversion and selectivity, respectively. (c) Catalytic performances of Co@C-H₂, Co@C-250Air-H₂ and Co@C-450Air-H₂ in chemoselective hydrogenation of 3-nitrostyrene to 3-aminostyrene. The black legends and red legends correspond to conversion and selectivity, respectively.

3.2 Catalytic results

At this point, the chemoselective hydrogenation of 3-nitrostyrene was chosen as the model reaction to study the catalytic properties of Co@C NPs and to see if the non-noble metal cobalt

nanoparticles can behave as a chemoselective catalyst. For testing this, the same reaction conditions that showed chemoselective hydrogenation when using noble metal catalysts, i.e. 120 °C and 7 bar of H₂ were selected.^{4,5} Notice that these are much milder conditions than those reported for the hydrogenation of 3-nitrostyrene with Co- and Fe-based catalysts.^{10,11} The reaction conditions and catalytic results are given in **Fig. 3**. It can be seen there that fresh Co@C NPs are active and selective catalyst for the hydrogenation of 3-nitrostyrene. When the conversion of 3-nitrostyrene is 95%, the selectivity to 3-aminostyrene is 93% which is comparable to the values obtained with noble metal catalysts.^{4,5} The initial TOF calculated based on surface Co atoms is ca. 8.2 h⁻¹ according to the particle size distribution of Co@C NPs. Notably, a reaction induction period of about 20-30 min can be observed in the kinetic curve (**Fig. S9**) when starting with the fresh catalyst that contains a core of metallic cobalt and a shell of CoOx. According with XPS results, this induction period could be caused by the time required for the reduction of surface CoOx to metallic Co under the reaction conditions. As presented in **Fig. S10**, the morphology and particle size distribution after the reduction under reaction conditions is similar to the fresh Co@C sample, suggesting that no structural changes or agglomeration has occurred. HRTEM images of the used sample also confirm that metallic Co NPs are still surrounded by carbon layers. Therefore, the above morphological characterization indicates that the nanoscale structures of the Co@C NPs sample is stable under reaction condition.

In a recent work, Zhang et al. have demonstrated that atomically dispersed Co species in the carbon matrix can serve as the active sites for oxidation reactions.³⁰ Herein, in order to exclude the role of atomically dispersed Co species in the hydrogenation reaction, we have also measured the residual solid after the acid leaching treatment (as shown in **Fig. S7**). No activity can be observed in the hydrogenation of 3-nitrostyrene, suggesting that the metallic Co NPs should be the active sites for hydrogenation reactions.

The recyclability of Co@C NPs in hydrogenation of 3-nitrostyrene was also tested. Since metallic Co NPs are paramagnetic, the separation of the solid catalyst from the liquid was very facile with the help of a magnetic bar^{31,32} (see **Fig. S11**). After washing several times with toluene, the catalyst can be reused without further treatments, and the Co@C catalyst shows good activity and selectivity for 5 cycles (see **Table S1**).

3.3 Role of the carbon layers in the catalyst

At this point, we know that the reduced Co@C NPs are active and chemoselective for reduction of substituted nitroarenes into corresponding anilines under mild reaction conditions. To investigate if the carbon layers play an intrinsic role for the chemoselective hydrogenation reaction, calcination of the Co NPs at 250 and 450 °C in air was performed to remove the carbon layers on the nanoparticles. The samples after calcination in air are denoted as Co@C-250Air and Co@C-450Air, respectively. From the Raman spectra (**Fig. S12**), we can find that in Co@C-250Air, bands at 1318 and 1595 cm^{-1} are still visible indicating that part of the carbon layers are still preserved. In Co@C-450Air, the above Raman bands are already very small suggesting that almost all the carbon layers have already been removed. As shown in **Fig. 3b**, it is possible to see that activity and selectivity drops when Co@C-250Air is used, while Co@C-450Air shows no activity in the hydrogenation reaction. The product distribution in the hydrogenation of 3-nitrostyrene with a Co@C-250Air sample as the catalyst is shown in **Fig. S13**. To explain these changes, TEM is used to clarify the structural transformation occurring with Co@C NPs after calcination in air. As shown in **Fig. S14**, metallic Co NPs crack into smaller CoOx NPs after the calcination in air at 250 °C, which has also been observed in other works.³³ The crystal lattice fringes of CoOx NPs can be observed in the HRTEM images, though, there are still some metallic Co NPs in the Co@C-250Air sample. Some carbon layers can still be found on Co-CoOx and CoOx NPs in Co@C-250Air, as was confirmed by Raman spectra. It should be noted that part of the carbon layers were burn during the calcination in air, resulting in the formation of naked Co and CoOx NPs.

In the Co@C-450Air sample (shown in **Fig. S15**), Co NPs are totally converted into Co_3O_4 NPs. The phase composition of the samples after calcination in air can also be measured by selective area electron diffraction (SAED). As can be seen in **Fig. S16**, metallic Co NPs transform into a mixture of Co and Co_3O_4 when calcined at 250 °C, and to pure Co_3O_4 when calcination was performed at 450 °C. Considering the significant decrease of activity observed when the Co@C sample was calcined at 250 °C and even more when temperature was 450 °C, it can be deduced that CoOx or Co_3O_4 cannot be the catalytically active phase.

Co@C, Co@C-250Air and Co@C-450Air NPs were reduced in the batch reactor under higher temperature and H_2 pressure (200 °C, 10 bar of H_2) before the hydrogenation reaction to reduce the

CoO_x species into metallic Co. After the reduction pre-treatment, 3-nitrostyrene was added and the hydrogenation reaction was performed at 7 bar of H₂ and 120 °C. As presented in **Fig. 3c**, the Co@C-H₂ gives a similar kinetic curve as the pristine Co@C except for the disappearance of the induction period due to the reduction pre-treatment. However, the situation changes a lot in the case of Co@C-250Air and Co@C-450Air. The Co@C-250Air-H₂ sample shows higher activity than pristine Co@C NPs and very good selectivity. This would indicate that the metallic Co NPs formed after reduction of Co@C-250Air should be responsible for the high activity and selectivity in hydrogenation reaction observed with Co@C-250Air-H₂. What's more, the reduction pre-treatment also has a significant effect on Co@C-450Air. After H₂ reduction, the Co@C-450Air-H₂ sample shows moderate activity and high selectivity, which further indicates that the chemoselective hydrogenation of 3-nitrostyrene is related with metallic Co and the role of carbon layers in Co@C NPs is mainly to protect Co NPs from over-oxidation by air.

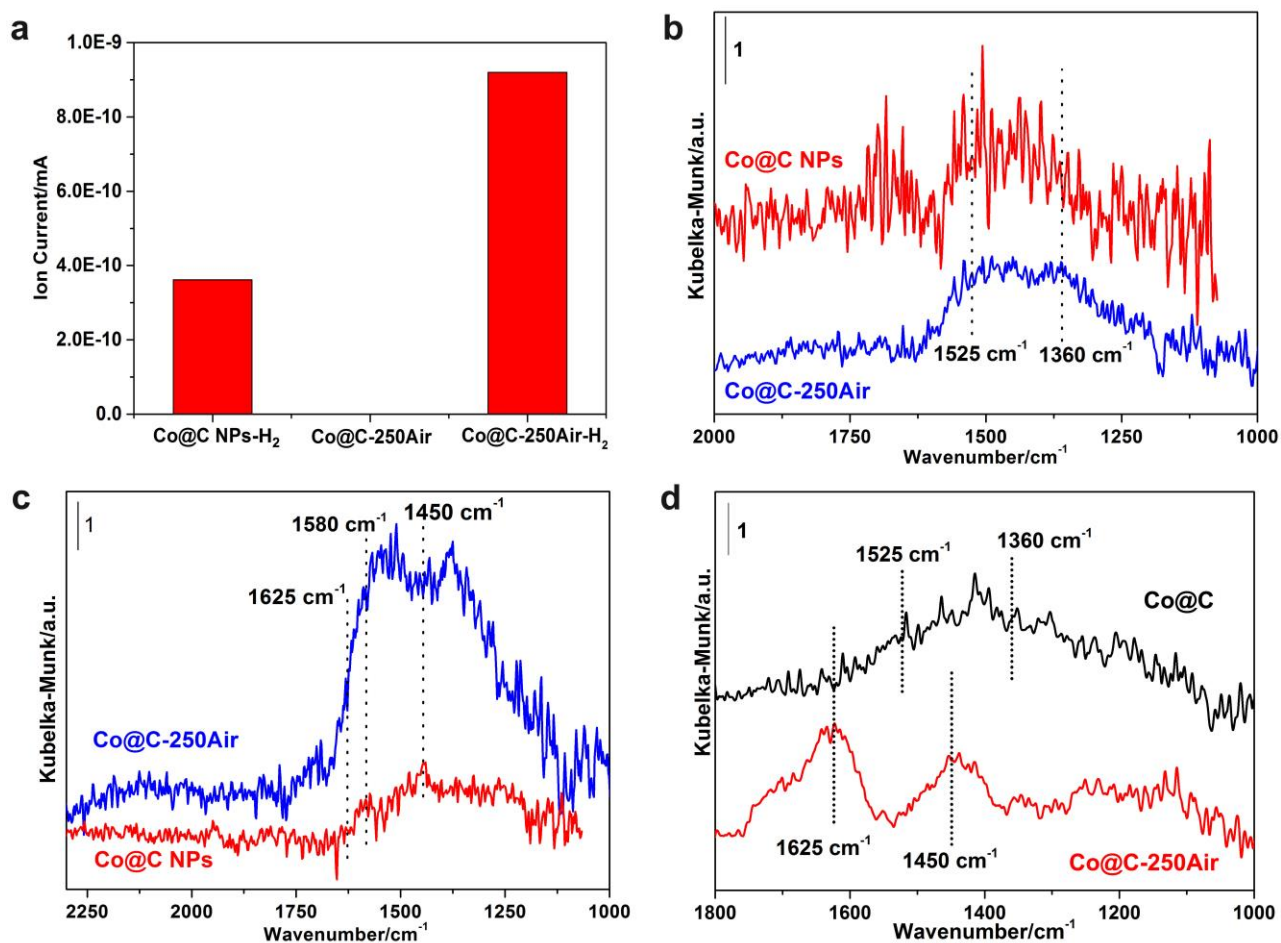


Fig. 4. H₂-D₂ exchange and DRIFTS adsorption experiments. (a) Enhancement of the ion current in mass signal of HD during the H₂-D₂ exchange experiment over Co@C-H₂, Co@C-250Air and

Co@C-250Air-H₂ NPs at 80 °C. (b) DRIFTS of adsorbed nitrobenzene, (c) DRIFTS of adsorbed styrene and (d) DRIFTS of co-adsorbed nitrobenzene and styrene on Co@C NPs and Co@C-250Air sample.

3.4 *In situ* adsorption spectroscopy study.

In order to explain the activity and high selectivity of Co@C NPs, H₂-D₂ exchange and the adsorption of substrates on Co@C NPs followed by diffuse reflectance infrared Fourier transform spectroscopy (DRIFTS) were carried out. The H₂-D₂ exchange rates on Co NPs and Co@C-250Air (with and without H₂ pre-reduction) are shown in **Fig. 4a**. H₂-D₂ exchange can be observed on Co@C NPs. Interestingly, as displayed in **Fig. S17**, a large amount of H₂ was released from Co NPs when the atmosphere was changed from H₂ to Ar after the *in situ* reduction process. The H₂ released should come from the H₂ adsorbed by Co NPs.^{34,35} It appears then that H₂ diffuses through the potential cracks present in carbon layers and it is activated on the surface of Co NPs. In the case of Co@C-250Air, no H₂-D₂ exchange can be observed when the sample is not pre-reduced. After H₂ pre-treatment, the H₂-D₂ exchange rate is higher on Co@C-250Air-H₂ than on Co@C suggesting that more Co sites are exposed after the removal of carbon layers and reduction of CoOx. The H₂-D₂ exchange experiments further confirm that metallic Co are the active sites for H₂ activation and carbon layers are not playing a direct role on the catalytic process.

We have found in previous work that the way that the reactant is adsorbed on metal catalysts can determine the chemoselectivity during hydrogenation of substituted nitroaromatics.³⁶ Then, in order to explain different catalytic behavior of Co@C NPs and Co@C-250Air samples for chemoselective hydrogenation of 3-nitrostyrene, we have performed *in situ* IR adsorption experiments by DRIFTS with nitrobenzene and styrene as probe molecules. For comparison, the IR spectra of nitrobenzene and styrene on KBr substrate have also been measured (see **Fig. S18**). The adsorption spectra of the probe molecules on Co@C and Co@C-250Air are shown in **Fig. S19**. The IR adsorption spectra of nitrobenzene on Co@C and Co@C-250Air samples show wide IR bands between 1600 cm⁻¹ to 1250 cm⁻¹ in both samples (see **Fig. 4b**). The vibration bands of -NO₂ groups can be observed at ca. 1525 cm⁻¹ and 1360 cm⁻¹.^{37,38} The intensity of the IR bands is similar on both samples suggesting that the adsorption spectra of Co@C and Co@C-250Air for nitrobenzene are similar. On the other hand, the

adsorption spectra of styrene on Co@C and Co@C-250Air (**Fig. 4e**) are significantly different. Indeed, as can be seen in **Fig. 4c**, the IR band corresponding to the aromatic ring can be observed between 1580 cm^{-1} and 1450 cm^{-1} , with the vibration mode of C=C bond at ca. 1625 cm^{-1} .³⁹ Co@C-250Air shows much stronger adsorption of styrene than Co@C sample, indicating that the adsorption of styrene on CoOx NPs will be enhanced when metallic Co NPs are oxidized. We have also studied the co-adsorption of nitrobenzene and styrene on Co@C and Co@C-250Air by DRIFTS. As can be seen in **Fig. 4d**, only the adsorption of nitrobenzene can be observed on Co@C, while a strong adsorption of styrene on Co@C-250Air occurs. In the case of Co@C-450Air, only the adsorption of styrene can be observed after the evacuation (see **Fig. S20**). Therefore, based on the IR adsorption results, we can conclude that the chemical states of Co have significant influences on the adsorption properties of substrate molecules in Co@C NPs. For metallic Co NPs, only $-\text{NO}_2$ groups will be preferentially adsorbed. In contrast, when the Co NPs are partially oxidized, the C=C instead of $-\text{NO}_2$ groups will be preferentially adsorbed. The selective adsorption observed in above experiments can explain the differences for the chemoselective hydrogenation of 3-nitrostyrene on metallic and partially oxidized cobalt nanoparticles.

3.5 Catalytic mechanism

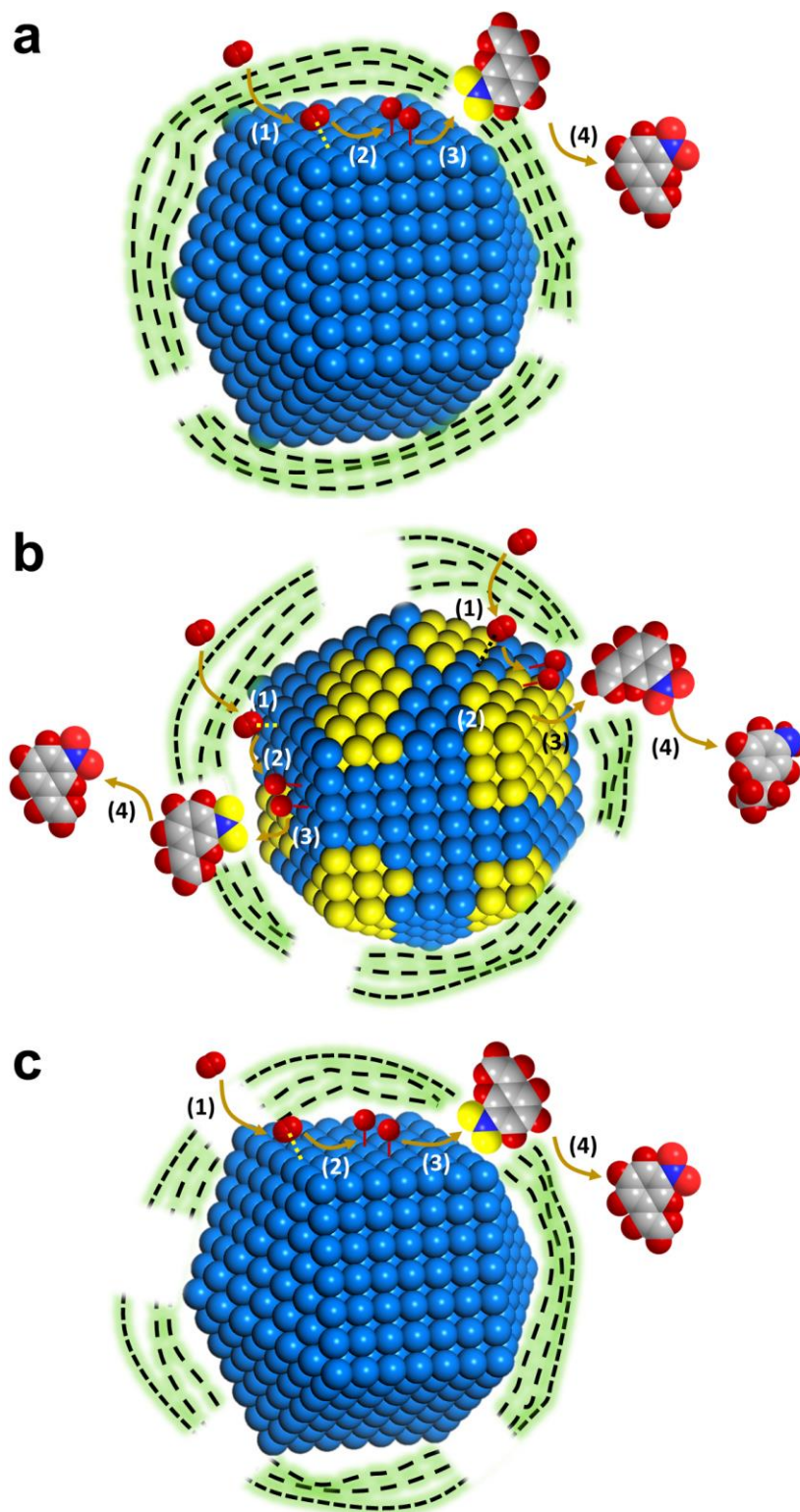


Fig. 5. Proposed reaction pathways of hydrogenation of 3-nitrostyrene on Co@C NPs with coverage of carbon layers (a) and defective coverage of carbon layers (b). In schematic illustration **Fig. 5a**, the chemoselective hydrogenation of $-\text{NO}_2$ groups can be divided into the following steps: the diffusion

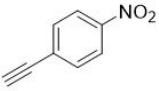
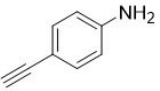
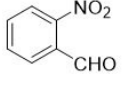
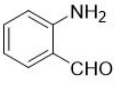
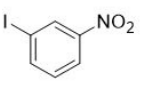
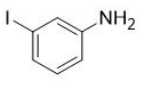
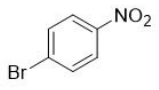
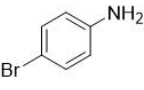
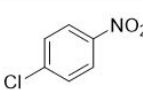
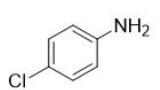
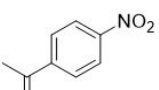
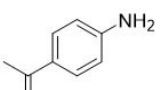
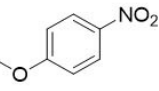
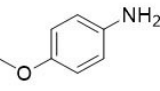
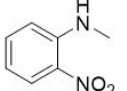
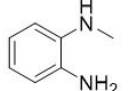
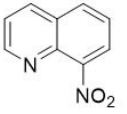
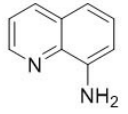
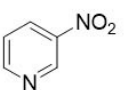
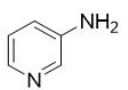
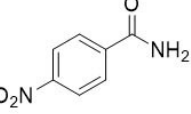
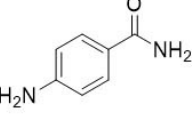
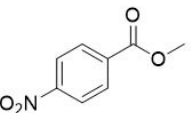
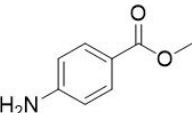
of H₂ from the gas phase up to the surface of metallic Co NPs (1), activation of H₂ (2), adsorption of the nitro aromatic (3), H-transfer from Co NPs to –NO₂ groups (4) for selective hydrogenation of –NO₂ groups. The scheme presented in **Fig. 5b**, sample with Co₃O₄ patches after removal part of carbon layers, hydrogenation of –NO₂ and =C groups can be divided into following steps, including the diffuse of H₂ to the surface of metallic Co NPs (1), activation of H₂ (2), hydrogen transfer (3) and hydrogenation of both –NO₂ and C=C groups (4). In schematic illustration **Fig. 5c**, for the *in situ* reduced sample after removal part of carbon layers, the chemoselective hydrogenation of –NO₂ groups can be divided into several steps, including the diffuse of H₂ to the surface of metallic Co NPs (1), activation of H₂ (2), H-transfer from Co NPs to –NO₂ groups (3) and selective hydrogenation of –NO₂ groups (4).

It appears then that unless Co nanoparticles are reduced to metallic nanoparticles, their activity and selectivity will be relatively low. In the case that partial (surface) oxidation occurs not only the hydrogenation activity is low, but also it will favor adsorption of styrene versus nitrobenzene, which can further favor the loss of chemoselectivity during the hydrogenation of 3-nitrostyrene.

Based on the above catalytic results and spectroscopic characterizations, we propose a reaction mechanism of chemoselective hydrogenation of 3-nitrostyrene on Co@C NPs covered by disordered carbon layers. Three cases with different oxidation state of Co and coverage of carbon layers are considered. As shown in **Fig. 5**, the first step in the hydrogenation reaction catalyzed by both Co@C and Co@C-250Air is the diffusion of H₂ to the surface of Co NPs under the cover of carbon layers. Then H₂ will be activated by Co NPs and form active H species. The third step will be different for Co@C and Co@C-250Air due to their different adsorption properties to the substrate molecules. In the case of Co@C (**Fig. 5a**), 3-nitrostyrene will be adsorbed on metallic Co preferentially through the –NO₂ groups, which will be reduced by the active H species formed on Co NPs. The adsorption of C=C bond on Co@C sample is relatively weak. However, in the case of Co@C-250Air (**Fig. 5b**), both C=C and –NO₂ group can have direct access to the surface of Co NPs. As a consequence, both –NO₂ and C=C groups can be hydrogenated by H₂, resulting in lower selectivity. When Co@C-250Air is reduced by H₂ before the catalytic test (**Fig. 5c**), more metallic Co sites will selectively absorb –NO₂ group instead of C=C bond, leading to high activity and selectivity.

3.6 Scope of the catalyst

Table 1. Scope of the hydrogenation of nitroarenes catalyzed by Co@C NPs. Reaction condition: Co@C NPs is 30 mg. 0.5 mmol nitroarenes, 30 μ L dodecane as the internal standard, 2 mL toluene as the solvent. †100 mg Co@C NPs as the catalyst. ‡2 mL THF as the solvent.

Entry	Substrate	Product	Time (h)	H ₂ pressure (bar)	Temp. (°C)	Con.	Sel.
1			6	7	120	93%	95%
2†			12	10	100	95%	95%
3			5	10	140	99%	97%
4			10	10	140	95%	99%
5			8	10	140	99%	97%
6			12	10	140	99%	95%
7			10	8	120	99%	99%
8			10	8	120	91%	93%
9			15	10	140	98%	95%
10			15	10	140	99%	95%
11‡			10	10	140	97%	99%
12			10	10	140	97%	99%

The scope of Co@C NPs in hydrogenation of substituted nitroarenes was investigated by reacting substituted nitrobenzene with halogens, amides, ester groups. In all cases, activity and chemoselectivity were high when working under mild reaction condition (**Table 1**). Selective hydrogenation of $-\text{NO}_2$ groups can be performed in the presence of groups such as olefins, alkynes and carbonyl under much lower H_2 pressure (7-10 bar) compared with previous reports (30-50 bar).¹⁰⁻¹² As it can be seen in **Table 1**, all the substrates can be selectively transformed with over 93% selectivity. Most of the entries show over 90% yield in the case of both electron-deficient and electron-rich substituents. Co@C NPs are also active and selective for nitroarenes with easily reducible moieties including alkyne, amide, ester, ketone and halogens. In previous work, the yields of heteroaromatic amines are not very high (from 53% to 75%). With Co@C NPs, we can get much higher yield of heteroaromatic amines (Entry 9 and 10 in **Table 1**). Thus, Co@C NPs are superior catalysts for chemoselective hydrogenation of nitroarenes under mild conditions.

4. Conclusions

In this work, we present a strategy for the synthesis of Co@C NPs. Metallic Co NPs are covered by thin carbon layers with small cracks. H_2 can diffuse through the cracks in the thin carbon layers and be activated at room temperature. The existence of carbon layers can protect the Co NPs from over-oxidation by air. This type of material shows good activity and selectivity for hydrogenation of nitroarenes with wide scope and good tolerance. They can also give high yields of heteroaromatic amines. The adsorption properties of substrate molecules will be affected by the chemical state of Co. Combining with *in situ* IR adsorption experiments and results from electron microscopy, a reaction mechanism is proposed in where the important role of metallic cobalt and the negative role of CoOx for the selective hydrogenation reaction is shown. And non-direct involvement of the carbon in the reaction is also proposed. The role of carbon layers is as protection of the Co NPs from getting deeply oxidized. This work provide new insights to design non-noble metal catalysts for heterogeneous catalytic applications.

Acknowledgements

L. L. thanks ITQ for a contract. The European Union is also acknowledged by ERC-AdG-2014-671093 — SynCatMatch. The authors also thank Microscopy Service of UVP for kind help on TEM and STEM measurements.

References

- [1] H.-U. Blaser, U. Siegrist, H. Steiner (Eds.), *Aromatic Nitro Compounds: Fine Chemicals Through Heterogeneous Catalysis*, Wiley-VCH, Weinheim, Germany, 2001.
- [2] A. Corma, P. Serna, *Chemoselective Hydrogenation of Nitro Compounds with Supported Gold Catalysts*, *Science*, 313 (2006) 332-334.
- [3] H.-U. Blaser, H. Steiner, M. Studer, *Selective Catalytic Hydrogenation of Functionalized Nitroarenes: An Update*, *ChemCatChem*, 1 (2009) 210-221.
- [4] A. Corma, P. Serna, P. Concepcion, J.J. Calvino, *Transforming nonselective into chemoselective metal catalysts for the hydrogenation of substituted nitroaromatics*, *J. Am. Chem. Soc.*, 130 (2008) 8748-8753.
- [5] P. Serna, M. Boronat, A. Corma, *Tuning the Behavior of Au and Pt Catalysts for the Chemoselective Hydrogenation of Nitroaromatic Compounds*, *Top. Catal.*, 54 (2011) 439-446.
- [6] J. Ran, J. Zhang, J. Yu, M. Jaroniec, S.Z. Qiao, *Earth-abundant cocatalysts for semiconductor-based photocatalytic water splitting*, *Chem. Soc. Rev.*, 43 (2014) 7787-7812.
- [7] H.R. Byon, J. Suntivich, Y. Shao-Horn, *Graphene-Based Non-Noble-Metal Catalysts for Oxygen Reduction Reaction in Acid*, *Chem. Mater.*, 23 (2011) 3421-3428.
- [8] R.V. Jagadeesh, H. Junge, M. Beller, *Green synthesis of nitriles using non-noble metal oxides-based nanocatalysts*, *Nat. Comm.*, 5 (2014) 4123.
- [9] B. Su, Z.C. Cao, Z.J. Shi, *Exploration of earth-abundant transition metals (Fe, Co, and Ni) as catalysts in unreactive chemical bond activations*, *Acc. Chem. Res.*, 48 (2015) 886-896.
- [10] F.A. Westerhaus, R.V. Jagadeesh, G. Wienhofer, M.M. Pohl, J. Radnik, A.E. Surkus, J. Rabeah, K. Junge, H. Junge, M. Nielsen, A. Bruckner, M. Beller, *Heterogenized cobalt oxide catalysts for nitroarene reduction by pyrolysis of molecularly defined complexes*, *Nat. Chem.*, 5 (2013) 537-543.
- [11] R.V. Jagadeesh, A.E. Surkus, H. Junge, M.M. Pohl, J. Radnik, J. Rabeah, H. Huan, V. Schunemann, A. Bruckner, M. Beller, *Nanoscale Fe₂O₃-based catalysts for selective hydrogenation*

of nitroarenes to anilines, *Science*, 342 (2013) 1073-1076.

[12] Z. Wei, J. Wang, S. Mao, D. Su, H. Jin, Y. Wang, F. Xu, H. Li, Y. Wang, In Situ-Generated $\text{Co}^0\text{-Co}_3\text{O}_4/\text{N}$ -Doped Carbon Nanotubes Hybrids as Efficient and Chemoselective Catalysts for Hydrogenation of Nitroarenes, *ACS Catal.*, 5 (2015) 4783-4789.

[13] T. Fu, M. Wang, W. Cai, Y. Cui, F. Gao, L. Peng, W. Chen, W. Ding, Acid-Resistant Catalysis without Use of Noble Metals: Carbon Nitride with Underlying Nickel, *ACS Catal.*, 4 (2014) 2536-2543.

[14] V. Berry, Impermeability of graphene and its applications, *Carbon*, 62 (2013) 1-10.

[15] J.S. Bunch, S.S. Verbridge, J.S. Alden, A.M. van der Zande, J.M. Parpia, H.G. Craighead, P.L. McEuen, Impermeable atomic membranes from graphene sheets, *Nano Lett.*, 8 (2008) 2458-2462.

[16] N. Fairley, CasaXPS Version 2.3.14, Casa Software Ltd, (2008).

[17] W. Zhong, H. Liu, C. Bai, S. Liao, Y. Li, Base-Free Oxidation of Alcohols to Esters at Room Temperature and Atmospheric Conditions using Nanoscale Co-Based Catalysts, *ACS Catal.*, 5 (2015) 1850-1856.

[18] M.R. Ward, E.D. Boyes, P.L. Gai, In Situ Aberration-Corrected Environmental TEM: Reduction of Model Co_3O_4 in H_2 at the Atomic Level, *ChemCatChem*, 5 (2013) 2655-2661.

[19] L. Qiu, J.Z. Liu, S.L. Chang, Y. Wu, D. Li, Biomimetic superelastic graphene-based cellular monoliths, *Nat. Commun.*, 3 (2012) 1241.

[20] J. Deng, P. Ren, D. Deng, X. Bao, Enhanced electron penetration through an ultrathin graphene layer for highly efficient catalysis of the hydrogen evolution reaction, *Angew. Chem. Int. Ed.*, 54 (2015) 2100-2104.

[21] S. Sun, C.B. Murray, Synthesis of monodisperse cobalt nanocrystals and their assembly into magnetic superlattices, *J. Appl. Phys.*, 85 (1999) 4325.

[22] S. Guo, S. Zhang, L. Wu, S. Sun, Co/CoO nanoparticles assembled on graphene for electrochemical reduction of oxygen, *Angew. Chem. Int. Ed.*, 51 (2012) 11770-11773.

[23] Y. Lu, X. Lu, B.T. Mayers, T. Herricks, Y. Xia, Synthesis and characterization of magnetic Co nanoparticles: A comparison study of three different capping surfactants, *J. Solid State Chem.*, 181 (2008) 1530-1538.

[24] X.Q. Zhao, S. Veintemillas-Verdaguer, O. Bomati-Miguel, M.P. Morales, H.B. Xu, Thermal

- history dependence of the crystal structure of Co fine particles, *Phys. Rev. B*, 71 (2005).
- [25] V.c.A. de la Peña O'Shea, P.R.r. de la Piscina, N. Homs, G. Aromí, J.L.G. Fierro, Development of Hexagonal Closed-Packed Cobalt Nanoparticles Stable at High Temperature, *Chem. Mater.*, 21 (2009) 5637-5643.
- [26] V.G. Hadjiev, M.N. Iliev, I.V. Vergilov, The Raman spectra of Co_3O_4 , *J. Phys. C: Solid State Phys.*, 21 (1988) L199-L201.
- [27] A.C. Ferrari, J. Robertson, Raman spectroscopy of amorphous, nanostructured, diamond-like carbon, and nanodiamond, *Phil. Trans. R. Soc. A*, 362 (2004) 2477-2512.
- [28] Y. Wang, D.C. Alsmeyer, R.L. McCreery, Raman spectroscopy of carbon materials: structural basis of observed spectra, *Chem. Mater.*, 2 (1990) 557-563.
- [29] V. Iablokov, S.K. Beaumont, S. Alayoglu, V.V. Pushkarev, C. Specht, J. Gao, A.P. Alivisatos, N. Kruse, G.A. Somorjai, Size-Controlled Model Co Nanoparticle Catalysts for CO_2 Hydrogenation: Synthesis, Characterization, and Catalytic Reactions, *Nano Lett.*, 12 (2012) 3091-3096.
- [30] L. Zhang, A. Wang, W. Wang, Y. Huang, X. Liu, S. Miao, J. Liu, T. Zhang, Co-N-C Catalyst for C-C Coupling Reactions: On the Catalytic Performance and Active Sites, *ACS Catal.*, 5 (2015) 6563-6572.
- [31] D. Wang, D. Astruc, Fast-growing field of magnetically recyclable nanocatalysts, *Chem. Rev.*, 114 (2014) 6949-6985.
- [32] M.B. Gawande, P.S. Branco, R.S. Varma, Nano-magnetite (Fe_3O_4) as a support for recyclable catalysts in the development of sustainable methodologies, *Chem. Soc. Rev.*, 42 (2013) 3371-3393.
- [33] H. Wang, C. Chen, Y. Zhang, L. Peng, S. Ma, T. Yang, H. Guo, Z. Zhang, D.S. Su, J. Zhang, In situ oxidation of carbon-covered cobalt nanocapsules creates highly active cobalt oxide catalysts for hydrocarbon combustion, *Nat. Commun.*, 6 (2015) 7181.
- [34] C.H. Bartholomew, R.C. Reuel, Cobalt-support interactions: their effects on adsorption and carbon monoxide hydrogenation activity and selectivity properties, *Ind. Eng. Chem. Prod. Res. Dev.*, 24 (1985) 56-61.
- [35] I.C. Yates, C.N. Satterfield, Intrinsic kinetics of the Fischer-Tropsch synthesis on a cobalt catalyst, *Energy Fuels*, 5 (1991) 168-173.
- [36] M. Boronat, P. Concepcion, A. Corma, S. Gonzalez, F. Illas, P. Serna, A Molecular mechanism

for the chemoselective hydrogenation of substituted nitroaromatics with nanoparticles of gold on TiO₂ catalysts: a cooperative effect between gold and the support, *J. Am. Chem. Soc.*, 129 (2007) 16230-16237.

[37] I. Ahmad, T.J. Dines, C.H. Rochester, J.A. Anderson, IR study of nitrotoluene adsorption on oxide surfaces, *Faraday Trans.*, 92 (1996) 3225.

[38] C.A. Koutstaal, P.A.J.M. Angevaere, E.J. Grootendorst, V. Ponec, On the Adsorption and Surface Reactions of Nitro- and Nitrosobenzene on Oxides: An IR Study, *J. Catal.*, 141 (1993) 82-93.

[39] B. Bachiller-Baeza, J.A. Anderson, FTIR and Reaction Studies of Styrene and Toluene over Silica-Zirconia-Supported Heteropoly Acid Catalysts, *J. Catal.*, 212 (2002) 231-239.